Real-time Imaging of Soft Tissues During Surgery, with Focus on Lumpectomy

Project report submitted

in partial fulfilment of the requirement for the degree of

Bachelor of Technology

By

KATHIR ILAKKIYAN S M	VISHAL KUMAR
200103125	200103123

DEPARTMENT OF MECHANICAL ENGINEERING

INDIAN INSTITUTE OF TECHNOLOGY GUWAHATI

APRIL, 2024

CERTIFICATE

This is to certify that the work contained in this project report entitled "**Real-time Imaging of Soft Tissues During Surgery, with Focus on Lumpectomy**" submitted by **Kathir Ilakkiyan S M (Roll No: 200103125)** and **Vishal Kumar (Roll No: 200103123)** to Indian Institute of Technology Guwahati towards the partial requirement of Bachelor of Technology in Mechanical Engineering is a bonafide work carried out by them under my supervision and that it has not been submitted elsewhere for the award of any degree.

(Dr. Kanagaraj S)
Project Supervisor

Date: April 2024
Place: Guwahati

DECLARATION

We declare that this written submission represents our ideas in our own words and where others' ideas or words have been included; we have adequately cited and referenced the sources. We also declare that we have adhered to all principles of academic honesty and integrity and have not misrepresented, fabricated or falsified any idea/data/fact/source in our submission. We understand that any violation of the above will be cause for disciplinary action by the institute and can also evoke penal action from the sources which have thus not been properly cited or from whom proper permission has not been taken when needed.

Kathir Ilakkiyan S M
(Roll No. 200103125)
Dept. of Mechanical Engineering

Vishal Kumar
(Roll No. 200103123)
Dept. of Mechanical Engineering

APPROVAL SHEET

This project report entitled "**Real-time Imaging of Soft Tissues during Surgery, with focus on Lumpectomy**" by **Kathir Ilakkiyan S M** and **Vishal Kumar** is approved for the degree of **Bachelor of Technology** in Mechanical Engineering.

Examiners
Dr. Rinku Kumar Mittal
Dr. Sachin S. Gautam

Supervisor
Dr. Kanagaraj S

Chairman
Dr. Manmohan Pandey

ABSTRACT

Real-time imaging of soft tissues during surgery, particularly lumpectomy, aims to provide a breakthrough advancement in the field of surgical medicine. This innovative approach uses multiple imaging technologies to provide surgeons with real-time, high-resolution images of soft tissues, enabling more precise and minimally invasive surgeries, especially for breast cancer, for which lumpectomy is a common treatment option. It ensures that the tumour is removed with high accuracy, reducing the risk of recurrence and improving the cosmetic outcome. In addition, the surgical procedure can be customised to meet the patient's individual needs. This research aims to identify the depth of tumour tissue from the breast skin, track the surgical tool during the procedure, and remove a minimum of healthy marginal tissue around the tumour tissue. Magnetic Resonance Images of breast tissues have been segmented to form 3D models for visualization and locating tumours. Zone-defining has been performed to cover the tumour mass completely using primitive shapes. A force feedback system has been devised to estimate the depth of the cancerous mass within the breast tissues. A tracking system has been combined with the force feedback system to provide better accuracy in the surgical process. Mathematical relations have been provided to estimate the tooltip location using optical reflective markers. The results have shown that the 3D models and zone-defining could highly improve the efficiency of the surgery. The force feedback system, along with the tracking system, could make the surgical process easier and enhance the accuracy and confidence of the surgeon.

Keywords: Lumpectomy, Segmentation, Zone-defining, Force feedback, Surgical tooltip tracking.

ACKNOWLEDGEMENT

Firstly, I owe my heartfelt gratitude and deepest regard to my supervisor, Dr. Kanagaraj S, Department of Mechanical Engineering, IIT Guwahati, India, for his relentless guidance, constant support and full cooperation throughout the project. His methods, vision and enthusiasm have always been a constant motivation and inspiration to me. Without his supervision and direction, this project could not have been a success.

Further, I would like to thank the PhD students, Mr. Arnob Dutta and Mr. Subhojit Jash, for their unwavering support, guidance and mentorship throughout the project.

CONTENTS

NOMENCLATURE

Latin Symbols

D	Distances from the optical reflective markers to the tooltip (mm)
a	x-coordinates of the optical reflective markers
b	y-coordinates of the optical reflective markers
c	z-coordinates of the optical reflective markers
x	x-coordinate of the tip of the surgical tool
y	y-coordinate of the tip of the surgical tool
z	z-coordinate of the tip of the surgical tool

Greek Symbols

Ω	ohm (unit of resistance)
μ	micro

Abbreviations

MRI	Magnetic Resonance Imaging
US	Ultra Sound
BCT	Breast Conservation Therapy
CT	Computed Tomography
AR	Augmented Reality
PA	Photo-Acoustic
RFITS	Real-time Fluorescence Imaging Topography Scanning
AFM	Atomic Force Microscopy
3D	3-Dimensional
FSR	Force Sensitive Resistor
CAD	Computer-Aided Design

LIST OF FIGURES

CHAPTER 1

INTRODUCTION

1.1 Background

Breast cancer is the most prevalent cause of cancer in women around the world, accounting for twenty-five percent of all female cancers. Breast cancer fatalities in South-East Asia are projected to climb to 61.7% by 2040 [1]. While Lung cancer was the most common cancer in men worldwide, contributing 15.4% of the total number of new cases diagnosed in 2020, breast cancer was the most common cancer in women worldwide, contributing 25.8% of the total number of new cases diagnosed in 2020[2]. The majority of the ladies were illiterate housewives aged 40 to 50. Most patients were married with more than three children. The majority of the patients were postmenopausal, and most of them had their menarche at the age of more than 13 years. In India, the rate of survival after five years for patients with local-stage cancer is 4.4 times higher than that of patients with distant-stage cancer. Furthermore, individuals over 65 had a 16% decreased likelihood of survival when compared to those between the ages of 15 and 39 [1, 3].

Sixty percent of palpable breast tumours in postmenopausal women are cancerous. About 10% of palpable tumours in women under 40 are malignant. Only when a breast lump reaches a size of roughly 2 to 3 cm can it be felt and detected with a self-breast inspection. Invasive Ductal Carcinoma is the most common type of breast cancer. Cancer starts in the milk ducts called ductal carcinoma in situ. It is referred to as invasive ductal carcinoma when it extends beyond the milk ducts into the surrounding tissues and lymph nodes. If the patient has a mastectomy or has their lymph nodes removed, the healing process takes a lot longer. Because of this, lumpectomy is a better option regarding recovery time and preserving the original appearance of the breasts [4].

Radiotherapy, chemotherapy, lumpectomy, and mastectomy are the common treatments for breast cancer depending on the risk level. A mastectomy involves removing the entire breast, including the cancerous tumour. Breast tissue is heavily lost as a result of this. Lumpectomy is a minimally invasive surgical procedure used to remove only cancerous tissues from the breast. Conventionally, Ultra Sound (US) imaging is used for intra-operative surgical guidance.

However, not all lesions are visible through the US. High-intensity radiation is used in radiotherapy, a cancer treatment, to shrink and kill cancer cells. The fundamental technique for employing medications and chemicals to destroy cancer cells is called chemotherapy [2, 5].

1.2 Motivation of the Study

Breast cancer has been a major concern in women's health for a long time. While mastectomy (removal of breast tissue as a whole including the cancer tumour) was the only solution for breast cancer, it posed a lot of problems for women in daily life including their self-respect and confidence. With the development of lumpectomy (surgery and removal of only the malignant tissues in the breast), it seemed much preferable for women as breast conservation therapy (BCT) could preserve the appearance of the breasts post-surgery [1, 2].

It is a huge honour to serve human health. This research has the potential to significantly benefit women's health. Although lumpectomy appears to be a better alternative to mastectomy, it is not without dangers. There is a higher risk of malignant tissues being overlooked during the surgical process, which could be life-threatening for the person undergoing surgery. A proper lumpectomy procedure or assistance should be provided to guarantee that all malignant tissues are removed while leaving the majority of healthy tissues intact. This can also boost the surgeon's confidence in his ability to perform a successful and efficient lumpectomy.

1.3 Objectives of the Study

The main objective of this study is to make the lumpectomy surgical process more efficient by minimizing the healthy tissues removed along with malignant tissues during surgery while maintaining a certain safe margin around them. Typically, lumpectomy is performed using pre-operative or intra-operative imaging tools to guide the surgical process. The clinician must remove the malignant tissues by utilising images generated as guidance. This study attempts to make the surgical operation less risky by making the surgical tool trackable in a three-dimensional environment. This study also intends to aid in the detection of the depth of a tumour within breast tissues. Finally, this study seeks to reduce the number of healthy tissues removed along with tumorous tissues by providing a commendable tracking system and a reasonably accurate depth detection approach. This research can have a significant impact on lumpectomy surgical approaches and lower the related risks, making the procedure easier to undertake.

1.4 Organization of the Thesis

This thesis has been organized in such a way the problems associated with the surgical procedure are provided at the beginning and continued with the possible solutions made to address those problems. **Chapter 1** focuses on the motive for carrying out the current work. It also provides background information on breast cancer removal methods, with a focus on lumpectomy and BCT. **Chapter 2** provides a literature assessment of significant research areas related to lumpectomy image guiding and surgical tool tracking procedures. **Chapter 3** describes the work's methodology and validation against existing literature. **Chapter 4** contains the results and explanations for the obtained results. In the final chapter, **Chapter 5**, the important findings and some future scopes are discussed.

CHAPTER 2

LITERATURE REVIEW

2.1 Image-guiding Techniques for Surgical Procedures

Ukimura and Gill's [6] study was focused on Ultrasound real-time imaging and synchronisation of the real-time US image with the higher resolution imaging of Computed Tomography (CT) or Magnetic Resonance Imaging (MRI). Augmented reality (AR) was used in laparoscopic surgery to project colours over tissues for better precision. The tracking was based on static images which were taken preoperatively and a **dynamic tracking system was not developed to perform the imaging of the surgery**.

Panasyuk et al. [7] performed research on creating a spectroscopic method that generates a map of a region of interest based on local biomarkers was used in this study. The study was focused on breast conservation therapy, specifically lumpectomy. A developed algorithm was created to distinguish cancer cells from healthy tissues. Through this paper, **only a static spectral image of tissues could be produced to assist surgeons**.

Han [8] made a review on the Photo-Acoustic (PA) imaging techniques used for spinal surgeries, photoacoustic tomography was used specifically for cancer detection and surgery. This technique produced live images during surgery whereas MRI/CT could produce only pre-operative images. One of the advantages of PA imaging over MRI/CT was that it had a higher imaging contrast and spatial resolution comparatively.

Chi et al. [9] made a review of the intraoperative optical molecular imaging technologies, focusing on contrast agents and surgical navigation systems, and then examined the prospects of multi-modality imaging technology for intraoperative imaging-guided cancer surgery. However, there were **limits in detecting depth in optical molecular imaging methods**, and more advancements from optical to multi-modality intraoperative imaging methods were needed to generate extensive and complete intraoperative applications.

Teatini et al. [10] assessed the benefits of intraoperative imagery for laparoscopic liver surgical navigation when displayed as augmented reality. There were significant disparities in AR accuracy thus favouring intraoperative imaging. Furthermore, the results revealed an effect of user-induced error: image-to-patient registration using clinician annotations resulted in 33% greater inaccuracy than image-to-patient registration algorithms that do not rely on user comments. Thus, to ensure correct surgical navigation for laparoscopic liver surgery, intraoperative imaging was recommended to adjust for deformation.

Farnia et al. [11] combined the PA imaging technique with the US imaging for higher contrast and resolution. In this process, registration of intra-operative PA images was done over pre-operative MR images. For recreating brain tissues, a brain-mimicking phantom was developed to assess the registration algorithm. However, a big limitation was that **the accurate combination of PA and MR required the development of a real-time and robust image registration algorithm**.

Quang et al. [12] created a Real-time Fluorescence Imaging Topography Scanning (RFITS) system that enabled multimodal optical imaging, CT-to-Optical image registration, and dynamic fiducial-free surgical navigation. The RFITS prototype was evaluated for system performance and tested in biological models for fluorescence-guided surgery. Multimodal imaging was performed on a life-sized human cranium model and image registration was investigated between intraoperative optical and preoperative tomographic data. Preclinical research demonstrated that the RFITS system could accurately guide multimodal surgeries.

2.2 Mechanical Properties of Tissues

Sirghi [13] and Lekka et al. [14] used Atomic Force Microscopy (AFM) to detect the interaction force between a microscopic tip and a sample surface. The AFM probe consists of a flexible cantilever with a sharp tip at its end. The force was sensed by a laser beam reflected by the top of the cantilever. Any small force acting on the tip deflects the cantilever and the laser beam; the deviation being measured by a photodiode. The cell stiffness was thus determined based on the force versus indentation curve that is usually obtained from the subtraction of deflections measured.

Li et al. [15] performed an AFM indentation study on breast cancer cells to determine the stiffness of the various cells. Benign human breast epithelial cells and malignant human breast epithelial cells were used in this study. The cells were analysed using a probing tool with different forces while plotting the graph of Young's modulus for every loading rate. It was observed that with the increase in loading rate, the elasticity linearly increased. It was concluded that irrespective of the loading rate, **the stiffness of the malignant tissues is always greater than normal tissues**.

Ramião et al. [16] applied mechanical compression load to various tissues to obtain the elasticity and to compare them. Mechanical testing of ex vivo breast tissues showed tumour tissues to have elasticity about 5 times the normal fat tissue and glandular tissue when 5% compression was applied. Magnetic Resonance Elastography for in vivo testing resulted in tumour tissues having 1.5-2 times higher elasticity with every frequency. The study concluded that the **tumour tissues are harder and stiffer than the normal tissues**.

Liu et al. [17] conducted a review of several cutting mechanisms utilised for soft tissue cutting using different blades. This study investigated four alternative cutting methods: incising, puncturing, shearing, and shaving. Soft tissue type, blade material, cutting parameters, and the amount of damage to the tissue sliced were the primary focus and classifications. Four cutting phases were discussed: deformation, rupture, intermediate, and steady.

2.3 Force Feedback Systems

Yeh et al. [18] used finite element simulation to create a piezoelectric actuator, which was then integrated into the master manipulator to provide thrust force against the user's finger pushing. If the indenter made contact with an object, the loading was used to modulate the thrust force of the piezoelectric actuator. This function can be expanded into a model of haptic perception, such as palpating an object. Instead of a human operator, this study employed a reciprocating mechanism to simulate finger pushing and tested the haptic feedback system under various contact situations. The findings indicated that the haptic feedback system may be utilised to determine the stiffness of objects.

Wang and Xu [19] synthesized a microinjection system which was driven by piezoelectric actuators. A strain gauge and piezoelectric actuators were put together to transfer the electrical signal into the movement or indentation of the injection tube and the pipette towards the experimental zebrafish embryo cells. The amount of force produced by the indentation on the cells was measured by a force sensor placed on the cells. The piezoelectric system ensures controlled and linear motion of the injector, unlike hand operation. Two controlled methods, namely, position control and force control, were used and it was observed that force control had a higher survival rate in the embryo cells.

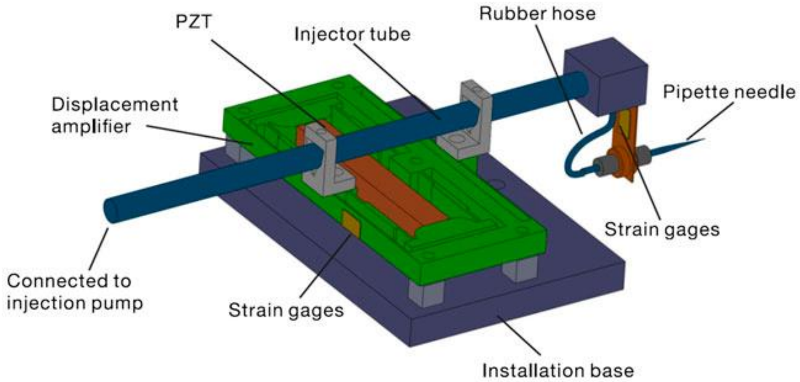

Figure 2.1: CAD model of the piezo-driven microinjection system [19]

Kun et al. [20] developed a resistance-based miniature force sensor to measure the force feedback. A flexible structure on the tip of the sensor generated the strain and the gauges attached to the tip recorded the strain. The gauges were connected to a Wheatstone bridge as variable resistors. Hence, the resistance variance in the gauges resulted in the output voltage in the bridge. This output was calibrated to the force needed to measure the feedback. Compared to previous developments, a sensor was developed that could measure in six dimensions. It was suitable for clinical purposes too, with proper size, modularity and protection.

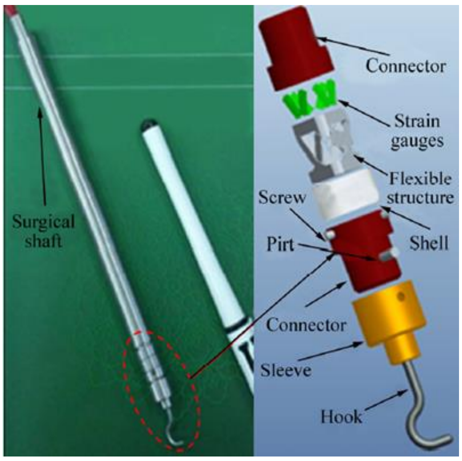

Figure 2.2: Assembly of the sensor in a surgical tool [20]

2.4 Motion Tracking Systems

Shin et al. [21] synthesized a 3D position-tracking system for the laparoscopic surgical tool. Five optical reflective markers were used at the end of the tool near the tooltip and were placed collinearly. Also, the probe had four spherical reflective markers for tracking. The actual distances between the markers were known and each marker was indexed from top to bottom. The laparoscopic instruments were extracted from the camera's photos using a high-level tracking algorithm.

Koeda et al. [22, 23] have developed a liver surgery tracking system for the surgical tool. The deformation of the liver was tracked along with the tool to track the surgical process accurately. Special markers were set on top of the knife, and the tip position was approximated by calibrating each marker and the knife tip location in advance. The discrepancy between the markers connected to the knife and the estimated knife-tip position was determined to be 0.3 mm.

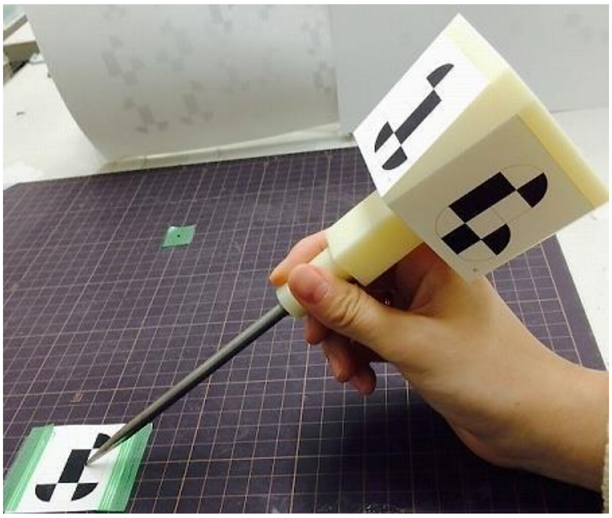

Figure 2.3: Pointed tool with markers attached to the top for locating the tip [22]

2.5 Research Gap

As evident from most of the Image-guided intraoperative techniques, the dynamic tracking of the internal soft tissues is yet to be properly studied and developed. Real-time visualization of the internal soft tissues needs to be researched further. A proper tracking algorithm should be developed and implemented to track intraoperative movements. Force feedback is not associated with lumpectomy surgery but is used for tissue stiffness comparison. Using force feedback in surgical tools could give a proper estimate of the depth of the tumour and could help in better positioning of the tool. Tracking along with force feedback can increase the precision of the surgery. Force fluctuation can be high during the cutting processes like incising and shearing. The force detected depends on various factors like the surgeon, the program created for force measurement, the cutting tool and the cutting angle. As the force feedback can be subjective to the clinician, a proper method has to be developed that can be used irrespective of these limiting factors.

CHAPTER 3

METHODOLOGY

3.1 Introduction

In this chapter, the works completed through this research project are discussed. Firstly, MR images of two breast cancer patients were segmented to create a 3D visualization of breast tissues and cancerous tissues within them. They were used as a base reference for the further proceedings of the project. That was continued by the study of force feedback and implementation in the surgical tool to measure the resistance produced by the silicone breast-mimicking phantom. Finally, a complete setup has been devised to incorporate tool tip tracking along with the force feedback in the surgical tool.

3.2 Processing MRI of Breast Tissues

To begin the project, segmentation of MR images of the breast tissues of two breast cancer patients was performed. Materialise Mimics image processing software was used to segment the MR images to form a 3D solid mass. The segmentation process can be seen in Figure 3.1.

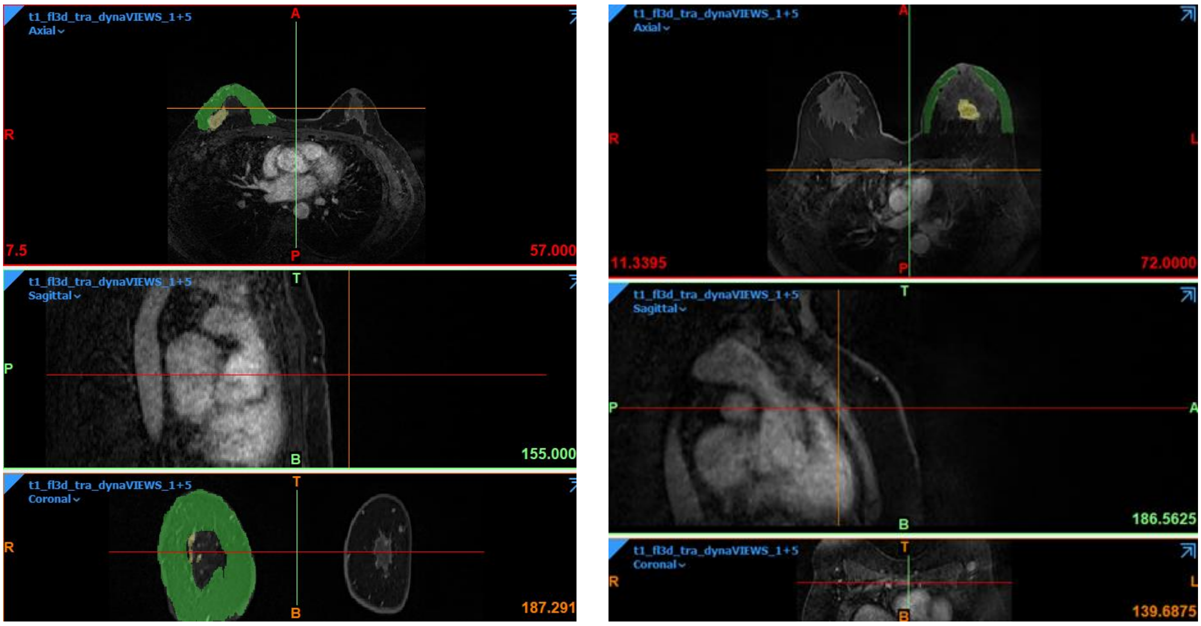

(a) (b)

Figure 3.1: Segmentation of breast tissues using Materialise Mimics image processing software for (a) Patient 1 and (b) Patient 2

After the segmentation process, the data was fed into another image processing software, Materialise 3-matic, to obtain optimized 3D models of the breast tissues distinguishing the malignant tissues from the healthy tissues. The models were further processed to get a smooth curvy surface. Figure 3.2 displays the 3D models of the two segmented breast tissues.

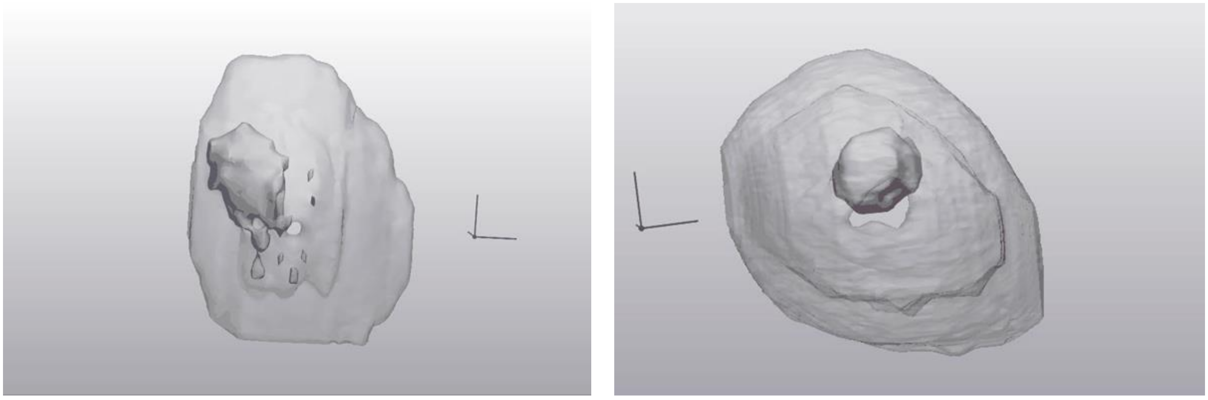

(a) (b)

Figure 3.2: (a) Heterogeneous mass in the upper outer quadrant of the right breast with satellite nodules, (b) Malignant mass lesion in retroareaolar and upper periareolar region of the left breast

Further, zone defining has been performed for the cancerous mass with satellite nodules shown in Figure 3.2 (a). Geomagic Design X software was used to provide zone defining using modifiable primitive shapes like spheres and cylinders for the various tumour tissues. The shape sizes are modifiable as per the surgeon’s requirements. Figure 3.3 shows the zone-defining method for the tumour mass.

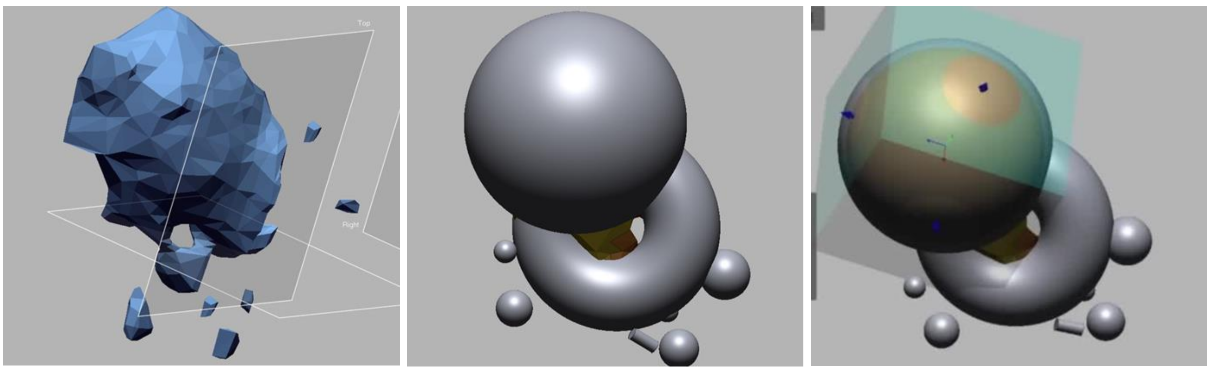

(a) (b) (c)

Figure 3.3: (a) Malignant mass with satellite nodules, (b) Zone defining using primitive shapes, (c) Shape modification

3.3 Force Feedback System

One of the next objectives is to estimate the depth of the tumourous mass within the breast tissues. This has been tackled by developing a force feedback system that provides an estimate of the resistance force provided by the breast tissues during incision. From the study conducted by Li et al. [15] and Ramião et al. [16], it was observed that the cancerous tissues had higher stiffness compared to the normal healthy tissues. This was the key observation that was used as the basis for developing a force feedback system. As the tumour is stiffer, the resistance force could be higher when the incision is made at that site. This change in force feedback could be used to estimate the depth of the tumour during the surgical process. The position of the breast tissues could be continuously changing as the tissues are primarily soft; hence, force feedback could be an alternative method for depth estimation as force is irrespective of the position of tissues.

A force sensor setup was made using the Tinkercad online circuit design platform. A Force Sensitive Resistor (FSR) was used to measure the force applied while the circuit was operated by an Arduino microcontroller. A 1 kΩ resistor and a 100 μF capacitor were used as a part of the circuit. The capacitor was used to stabilize the force feedback results from the sensor. The online circuit has been replicated with an actual Arduino setup and an FSR which can measure mass in a range of 100 g to 20 kg. Figure 3.4 demonstrates the (a) model made using Tinkercad and the (b) actual force sensor setup.

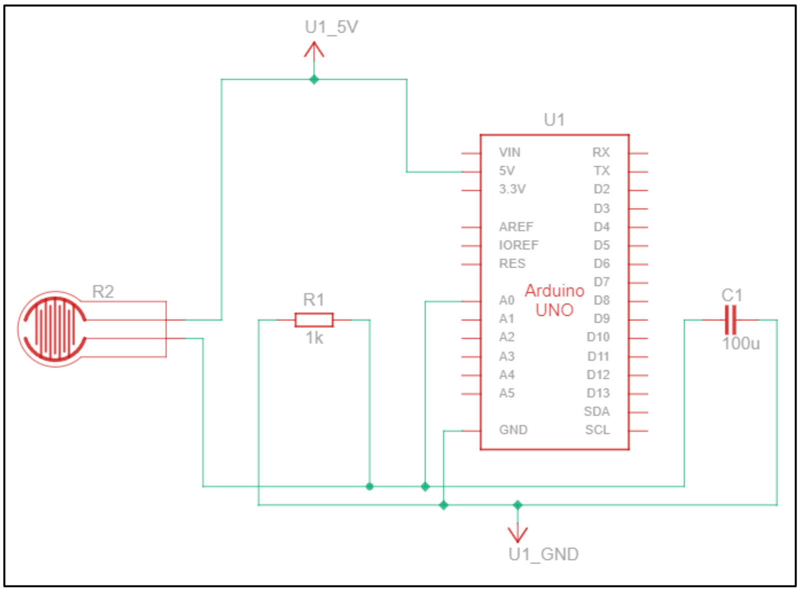

(a)

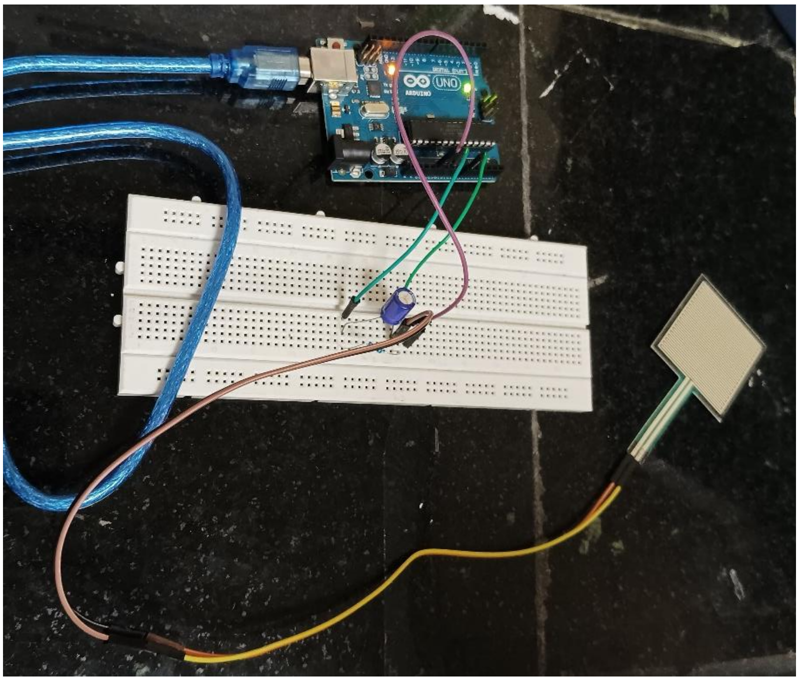

(b)

Figure 3.4: (a) Force feedback circuit made using Tinkercad, (b) Actual force feedback setup that replicates the Tinkercad circuit

The Arduino code used for the functioning of the force feedback setup is shown below. A calibration factor of 0.314 has been calculated for the FSR using multiple known weights. The final force output has been calculated using this calibration factor. The force feedback could be obtained in both mass and force units, namely, kilogram and newton.

```
float cf = 0.314; //Calibration factor (0.314)
int Reading=0;
float vout;
void setup() {
  Serial.begin(9600);
}

void loop() {
  Reading = analogRead(A0);
  vout = (Reading*5.0)/1023.0;
  vout = vout*cf;
  Serial.print("Force Sensor Reading = ");
  Serial.print(vout,3);
  Serial.print(" kg, ");
  Serial.print(vout*9.81,3);
  Serial.print(" N, calibration factor = ");
  Serial.print(cf,3);
  Serial.println("");
  delay(500);
}
```

To carry out the force feedback testing, a model of the breast and the tumour tissues inside was required. Silicone rubber Grade LSR 120 was chosen for the breast tissue material and a rubber piece was used for the tumour tissue, as rubber had a stiffer physical property than silicone. A cubic mould was made using acrylic sheets to create silicone casting.

The dimensions of the silicone cube were 50 mm x 50 mm x 40 mm (length x breadth x height) and the dimensions of the rubber were 30 mm x 20 mm x 10 mm. The casting was left undisturbed for 24 obtain a flexible solid silicone phantom. Figure 3.5 shows the rubber casting made to mimic the breast tissues.

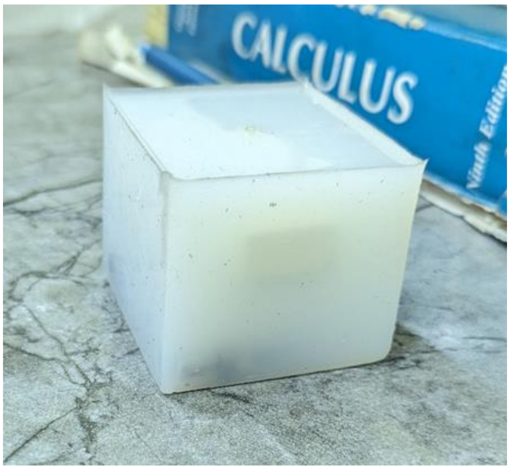

Figure 3.5: Silicone rubber casting with a stiffer rubber material inside mimicking the cancerous mass.

3.4 Surgical Tool Tip Estimation

Along with the force feedback, to make the surgery more accurate, the tip of the surgical tool has to be tracked. A scalpel has been used as a basic surgical tool to create a tool-tracking model. A CAD model has been developed that could be 3D printed to be fixed to the scalpel head. The model has been developed in such a way as to place optical reflective markers to estimate the tip of the tool by using mathematical relations. Figure 3.6 shows the CAD model developed to be 3D printed. A mathematical relation has been made to compute the tip of the scalpel using three known coordinates of the reflective markers in the 3D space. Figure 3.7 demonstrates the coordinates of the markers and the measurements to the tooltip.

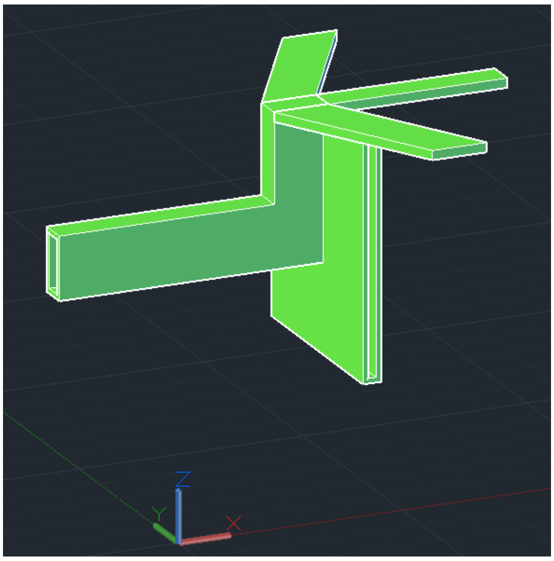

Figure 3.6: CAD model of the tracker that could be inserted on the tool head. Optical markers could be placed on the three hands above.

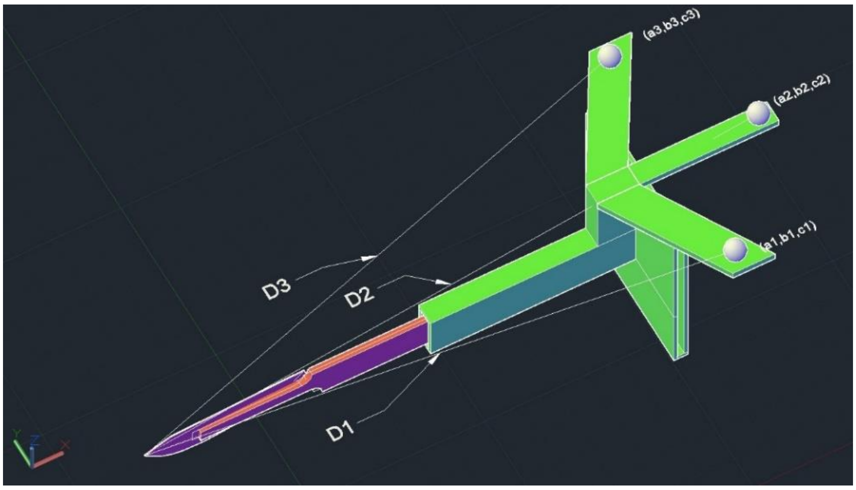

Figure 3.7: Coordinates of the optical markers and the respective distances to the tooltip

As shown in Figure 3.7, the three optical markers were coordinated in the 3D space as (a_1,b_1,c_1), (a_2,b_2,c_2) and (a_3,b_3,c_3), and their respective distances to the tip are denoted by D_1, D_2 and D_3. The coordinate of the tip can be calculated using the equations from 3.1.

$$(x - a_1)^2 + (y - b_1)^2 + (z - c_1)^2 = D_1^2 \tag{3.1a}$$

$$(x - a_2)^2 + (y - b_2)^2 + (z - c_2)^2 = D_2^2 \tag{3.1b}$$

$$(x - a_3)^2 + (y - b_3)^2 + (z - c_3)^2 = D_3^2 \tag{3.1c}$$

The three equations could be solved to obtain x, y and z. These three points would give the coordinates of the tooltip. To make the operation faster, a MATLAB code has been devised to obtain the tooltip coordinates based on the coordinates of the optical markers. The distances D_1, D_2 and D_3 would be fixed and they have to be calibrated to the tracking system each time before the operation for accurate tracking.

```
q = points - points(3,:);

e = null(q)'*sqrt(norm(q(1,:))*norm(q(2,:)));%vector normal to plane
trans = (1/3)*sum(points) + e;
p_translated = points - trans;                % translate

w = sum(p_translated.*p_translated,2)-distance.^2;
q1 = p_translated\ones(3,1);
qw = p_translated\w;
A = roots([q1'*q1, (2*qw'*q1-4), qw'*qw]);   % A = snew dot snew
snew = (1/2)*(q1*A.' +qw)';                   % one row of (x,y,z)
tip_coordinates = snew + trans;
```

The above code could provide the tooltip coordinates if the coordinates of the three optical markers and the distances to the tip were given as input. The distances were fixed throughout, hence only one initial input would be required. Whereas, coordinates of the markers were to be provided continuously when in operation.

3.5 Integrating Force Feedback with Tool Tracking

Finally, the tool tracking and force feedback systems if put together could complete the study producing efficient surgical assistance. Flat surfaces with a slit space can be seen in the model developed for tool tracking as shown in Figure 3.6. That space could be utilized to place the FSR sensor during the operation. The resistive force on the scalpel could be directly transmitted to the FSR to obtain the force feedback. This way, the user's subjective interference with the force results could be completely avoided. Figure 3.8 displays the (a) 3D printed model of the tracking and force feedback setup and the (b) model along with the scalpel inserted in it.

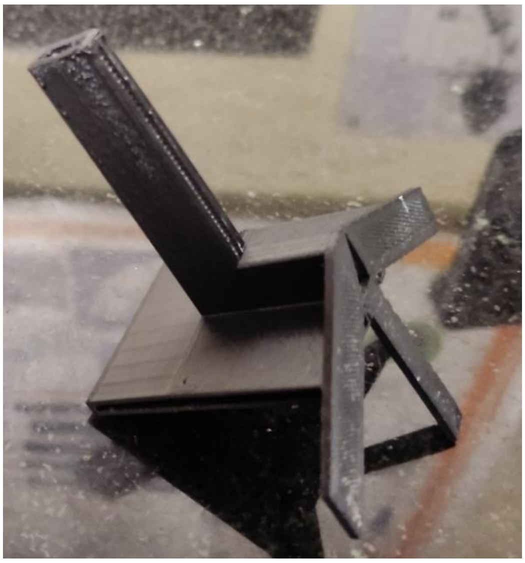

(a)

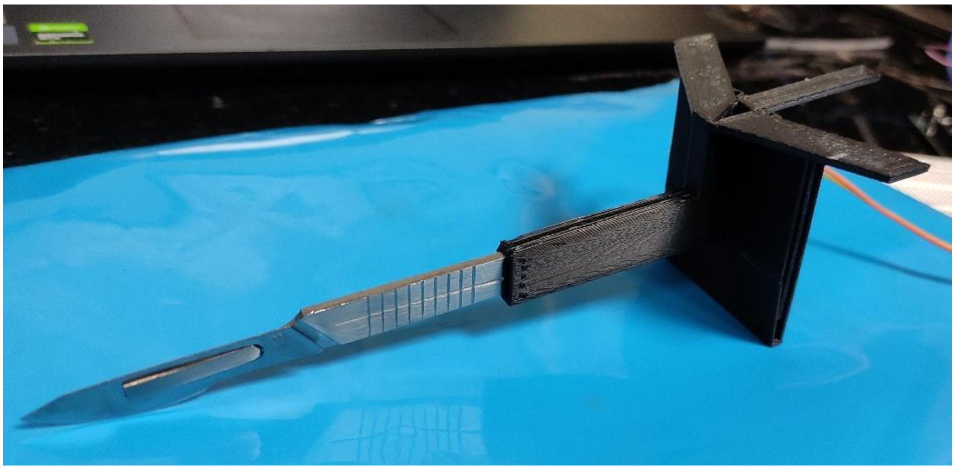

(b)

Figure 3.8: (a) 3D printed model of the CAD model shown in Figure 3.6, (b) The model shown in (a) along with the scalpel inserted in it.

The user could hold the end of the model while operating without the tool slipping out. Both the tracking and force feedback systems have been integrated using the same 3D model. The force feedback readings have been taken while operating the scalpel on the silicone rubber casting. The readings were noted while making an incision far and away from the rubber piece, just on the silicone, and while making an incision close to the rubber and towards it. These readings were tabulated and compared to display the differences in force feedback when acted on different materials. Figure 3.9 displays the (a) whole setup of tracking and force feedback systems, and the (b) operation of the tool by a user. Figure 3.10 demonstrates the two-incision types.

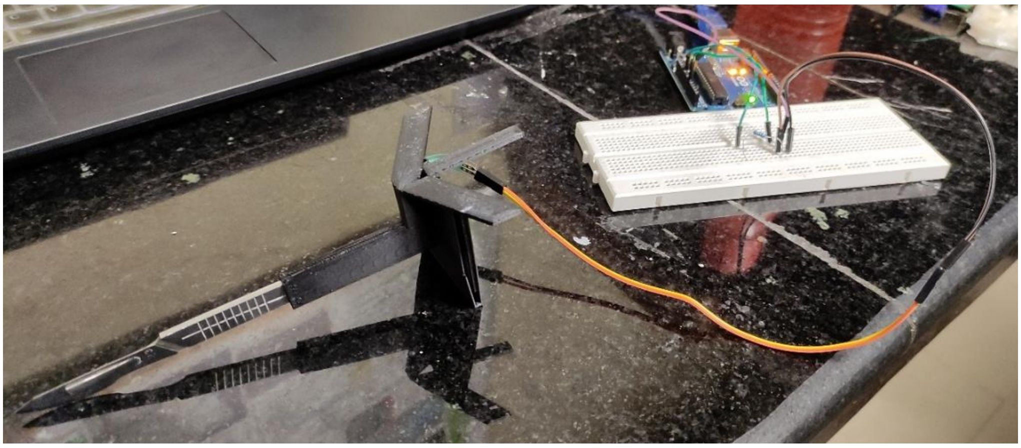

(a)

(b)

Figure 3.9: (a) The complete setup with integrated tracking and force feedback system, (b) Operating the surgical tool on the silicone casting while measuring the force response.

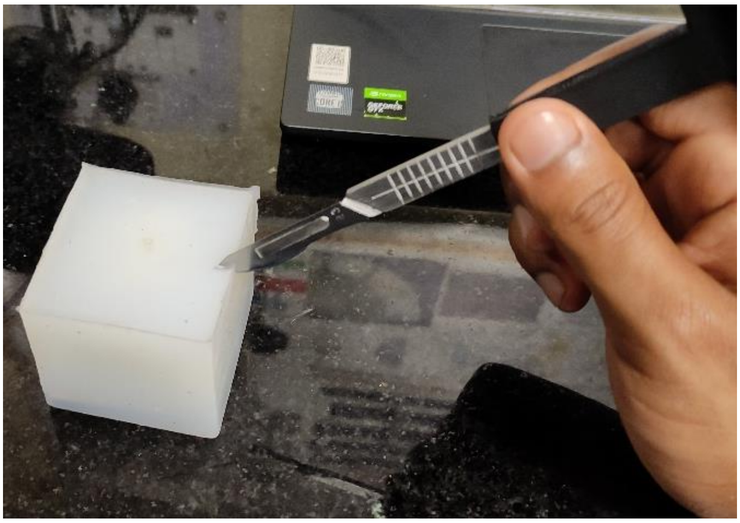

(a)

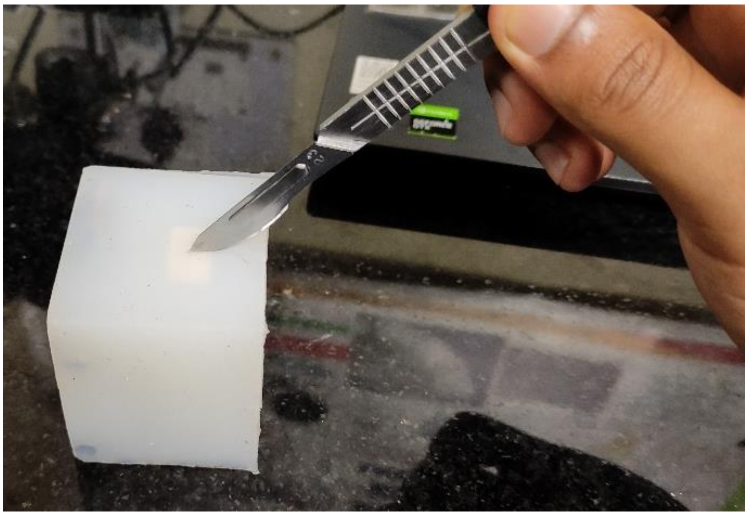

(b)

Figure 3.10: Measurement of resistive force by making incisions (a) far from the rubber piece and (b) towards the rubber piece

CHAPTER 4

RESULTS AND DISCUSSION

4.1 MRI Segmentation and Zone Defining

The MR images were successfully segmented and 3D models of breast tissues were obtained for both sets of MRI. The models depicted the actual breast tissues pretty accurately. The MRI segmentation and zone-defining processes were to be completed well in advance of the surgical operation. Zone defining would be completely subjective to each patient and their cancerous mass. Zone-defining complications vary from one to another. If the cancerous mass were to be just a spherical lump, it could be quite easy to define the area with a sphere of a certain diameter, but if the same mass had an irregular shape with multiple satellite nodules, zone-defining could get very complicated and hard for the surgeon to follow.

4.2 Tracking of the Surgical Tool

Though a tracking algorithm has not been developed, a mathematical relation as well as the MATLAB code to obtain the tooltip coordinates have been properly devised. The algorithm would just need to measure the coordinates of the three optical reflective markers in the 3D space. This would require the use of infrared cameras to capture the live locations of the markers. The MATLAB code was run with a set of positions of the markers and the respective distances to the tooltip. These input data were taken from the CAD model in Figure 3.7 and they were used in the main code as given below.

```
points = [109.32 26.72 67.71;
          134.07 59.70 67.71;
          109.32 92.68 67.71];
distance = [157.70 178.75 157.70]';
```

Using these input data, the location of the tooltip was estimated through the output as,

```
tip_coordinates =
  -43.3546   59.7000   45.9824
  -43.3546   59.7000   89.4376
```

Two results were obtained for the position of the tooltip. The reason for this would be, that if three points are in the same plane and three distances are given forming three spheres respectively, there could be two resulting points that intersect the three spheres. But, as the tooltip would be below the plane of the markers during the surgical process, the first result can be taken as the correct location of the tooltip. If the algorithm were to be made for the 3D space, the coordinates could be fed into the system to locate the tooltip accurately.

4.3 Force Feedback System

The FSR sensor has been perfectly placed in the slit provided in the 3D tracking model. The resistive force produced by the silicone casting has been measured at two different locations, at the edge of the silicone rubber far from the rubber piece, and in the middle of the silicone towards the rubber piece. The results were tabulated and the force feedback in both cases is compared graphically in Figure 4.1.

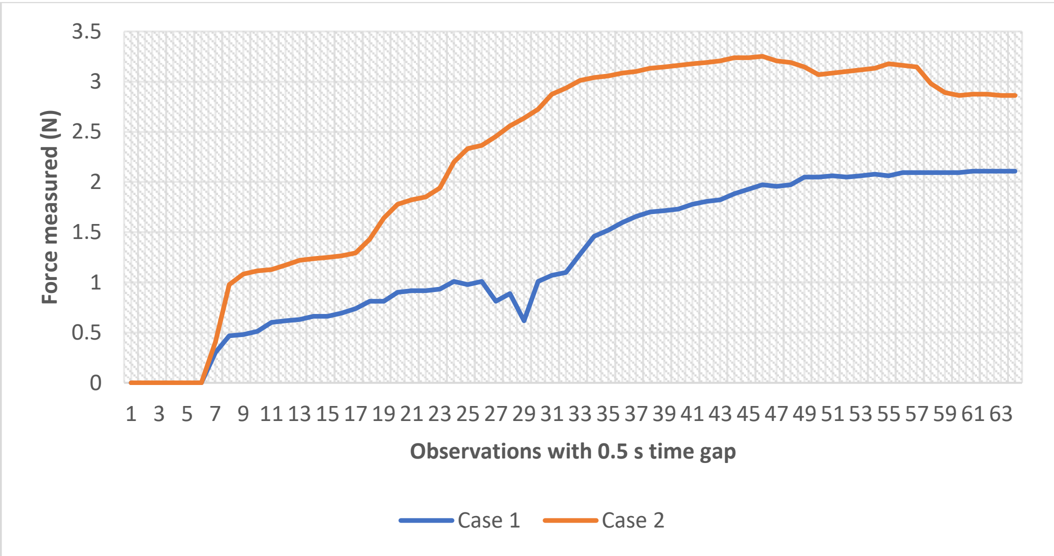

Figure 4.1: The resistive force on the incision is graphically presented by comparing the two cases. Case 1 represents the incision made far from the rubber and Case 2 represents the incision made close to the rubber.

From Figure 4.1, it is understandable that for case 2 the resistive force was higher throughout as the incision was made at the hard rubber site while case 1 was at the soft silicone site. When the cut was made through the silicone surface in case 1, a sudden reduction in the force level was measured as the resistance would have been less just after the cut was made.

CHAPTER 5

CONCLUSION AND FUTURE SCOPES

5.1 Key Findings

The study has been completed with a few key findings from the experiments performed to improve the efficiency of the lumpectomy surgical procedure. The conclusions are as follows:

- The segmentation and 3D modelling of MR images of the breast tissues of the patients could immensely aid the surgeon with the visualization of the cancerous mass and the exact location inside the breast.
- The zone-defining process could further help the surgeon to plan the shape of the cut. This could help in minimizing the extra healthy tissues that could be unnecessarily removed.
- The surgical tool could be tracked in the 3D space by using the relation between the optical markers and the tooltip. This could greatly improve the accuracy and the confidence of the surgeon.
- The resistive force feedback system has shown a difference in the results with the changes in the point of incision. The stiffer the material, the higher the force feedback. This proves that the depth could be quite accurately measured if this system is used intra-operatively during the lumpectomy surgery. The results have also proved that the concept of FSR fixed behind the tool could provide precise readings.

5.2 Scopes for Future Work

The present study can be further developed by enhancing each of the above-mentioned components. The following works can be performed to proceed with this work into a proper medical advancement.

- Registration of the 3D model created by segmenting the MR images could be done in the 3D space by further developing the tracking system.
- Zone-defining could be made more accurate by incorporating better shapes that could closely trace the shape of the cancerous mass.
- The mathematical relation is made but a robust 3D tracking algorithm could be devised to complete the work in this part.
- The force feedback setup can be made less cumbersome by incorporating smaller FSR and modifying the feedback setup.

REFERENCES

1. Sathishkumar, Krishnan, Jayasankar Sankarapillai, Aleyamma Mathew, Rekha A. Nair, Nitin Gangane, Sushma Khuraijam, Debabrata Barmon et al. "Breast cancer survival in India across 11 geographic areas under the National Cancer Registry Programme." Cancer (2024).

2. Łukasiewicz, Sergiusz, Marcin Czeczelewski, Alicja Forma, Jacek Baj, Robert Sitarz, and Andrzej Stanisławek. "Breast cancer—epidemiology, risk factors, classification, prognostic markers, and current treatment strategies—an updated review." Cancers 13, no. 17 (2021): 4287.

3. Kerketta, Zenith H., Anit Kujur, Neelanjali Kumari, Vidya Sagar, F. N. U. Pushpa, Zenith Kerketta, N. E. E. L. A. N. J. A. L. I. KUMARI Sr, and PUSHPA PUSHPA. "A Cross-Sectional Study on the Epidemiology of Newly Diagnosed Breast Cancer Patients Attending Tertiary Care Hospitals in a Tribal Preponderant State of India: Regression Analysis." Cureus 15, no. 6 (2023).

4. Scholl, Ashley Rose, and Melina B. Flanagan. "Educational case: invasive ductal carcinoma of the breast." Academic Pathology 7 (2020): 2374289519897390.

5. Gittleman, Mark A. "Single-step ultrasound localization of breast lesions and lumpectomy procedure." The American journal of surgery 186, no. 4 (2003): 386-390.

6. Ukimura, Osamu, and Inderbir S. Gill. "Imaging-assisted endoscopic surgery: Cleveland Clinic experience." Journal of endourology 22, no. 4 (2008): 803-810.

7. Panasyuk, Svetlana V., Shi Yang, Douglas V. Faller, Duyen Ngo, Robert A. Lew, Jenny E. Freeman, and Adrianne E. Rogers. "Medical hyperspectral imaging to facilitate residual tumor identification during surgery." Cancer biology & therapy 6, no. 3 (2007): 439-446.

8. Han, Seung Hee. "Review of photoacoustic imaging for imaging-guided spinal surgery." Neurospine 15, no. 4 (2018): 306.

9. Chi, Chongwei, Yang Du, Jinzuo Ye, Deqiang Kou, Jingdan Qiu, Jiandong Wang, Jie Tian, and Xiaoyuan Chen. "Intraoperative imaging-guided cancer surgery: from current fluorescence molecular imaging methods to future multi-modality imaging technology." Theranostics 4, no. 11 (2014): 1072.

10. Teatini, Andrea, Egidijus Pelanis, Davit L. Aghayan, Rahul Prasanna Kumar, Rafael Palomar,

Åsmund Avdem Fretland, Bjørn Edwin, and Ole Jakob Elle. "The effect of intraoperative imaging on surgical navigation for laparoscopic liver resection surgery." Scientific Reports 9, no. 1 (2019): 18687.

11. Farnia, Parastoo, Bahador Makkiabadi, Maysam Alimohamadi, Ebrahim Najafzadeh, Maryam Basij, Yan Yan, Mohammad Mehrmohammadi, and Alireza Ahmadian. "Photoacoustic-MR image registration based on a co-sparse analysis model to compensate for brain shift." Sensors 22, no. 6 (2022): 2399.

12. Quang, Tri T., Wei F. Chen, Francis A. Papay, and Yang Liu. "Dynamic, real-time, fiducial-free surgical navigation with integrated multimodal optical imaging." IEEE photonics journal 13, no. 1 (2020): 1-13.

13. Sirghi, Lucel. "Atomic force microscopy indentation of living cells." Microscopy: science, technology. Applications and Education, Formatex, Badajoz (2010): 433-440.

14. Lekka, Małgorzata, Dorota Gil, Katarzyna Pogoda, Joanna Dulińska-Litewka, Robert Jach, Justyna Gostek, Olesya Klymenko et al. "Cancer cell detection in tissue sections using AFM." Archives of biochemistry and biophysics 518, no. 2 (2012): 151-156.

15. Li, Q. S., Gabriel YH Lee, Choon Nam Ong, and Chwee T. Lim. "AFM indentation study of breast cancer cells." Biochemical and biophysical research communications 374, no. 4 (2008): 609-613.

16. Ramião, Nilza G., Pedro S. Martins, Rita Rynkevic, António A. Fernandes, Maria Barroso, and Diana C. Santos. "Biomechanical properties of breast tissue, a state-of-the-art review." Biomechanics and modeling in mechanobiology 15 (2016): 1307-1323.

17. Liu, Zhihua, Chengyong Wang, Zhihua Chen, and Jianbo Sui. "The advance of surgical blades in cutting soft biological tissue: A review." The International Journal of Advanced Manufacturing Technology 113 (2021): 1817-1832.

18. Yeh, Chien-Hsien, Fong-Chin Su, Yan-Shen Shan, Marat Dosaev, Yury Selyutskiy, Irina Goryacheva, and Ming-Shaung Ju. "Application of piezoelectric actuator to simplified haptic feedback system." Sensors and Actuators A: Physical 303 (2020): 111820.

19. Wang, Guangwei, and Qingsong Xu. "Design and development of a piezo-driven microinjection system with force feedback." Advanced Robotics 31, no. 23-24 (2017): 1349-1359.

20. Li, Kun, Bo Pan, Wen-peng Gao, Hai-bo Feng, Yi-li Fu, and Shu-guo Wang. "Miniature 6-axis force/torque sensor for force feedback in robot-assisted minimally invasive surgery." Journal of Central South University 22, no. 12 (2015): 4566-4577.

21. Shin, Sangkyun, Youngjun Kim, Hyunchul Cho, Deukhee Lee, Sehyung Park, Gerard Jounghyun Kim, and Laehyun Kim. "A single camera tracking system for 3D position, grasper angle, and rolling angle of laparoscopic instruments." International journal of precision engineering and manufacturing 15 (2014): 2155-2160.

22. Koeda, Masanao, Daiki Yano, Mayuko Doi, Katsuhiko Onishi, and Hiroshi Noborio. "Calibration of surgical knife-tip position with marker-based optical tracking camera and precise evaluation of its measurement accuracy." J. Bioinform. Neurosci.(JBINS) 4, no. 1 (2018): 155-159.

23. Yano, Daiki, Mayuko Doi, Masanao Koeda, Kodai Okumoto, Shogo Yoshida, Katsuhiko Onishi, Hiroshi Noborio, and Kaoru Watanabe. "Verification of accuracy of knife tip position estimation in liver surgery support system." In 2017 International Conference on Intelligent Informatics and Biomedical Sciences (ICIIBMS), pp. 284-285. IEEE, 2017.